sustainability

MDPI

Article

P2P Coordinated Control between SPV and STATCOM in a Microgrid for Power Quality Compensation Using LSTM–Genetic Algorithm

Durgamadhab Swain [1,2], Meera Viswavandya [3], Ritesh Dash [4], Kalvakurthi Jyotheeswara Reddy [4], Dhanamjayulu Chittathuru [5,*], Arunkumar Gopal [5], Baseem Khan [6,*] and Manam Ravindra [7]

1 Research Scholar, Department of Electrical Engineering, Biju Patnaik University of Technology, Rourkela 769015, India; durgamadhab17@gmail.com
2 Department of Electrical Engineering, Ajay Binay Institute of Technology, Cuttack 753014, India
3 Department of Electrical Engineering, Odisha University of Technology and Research, Bhubaneswar 751029, India; mviswavandya@outr.ac.in
4 School of Electrical and Electronics Engineering, REVA University, Bengaluru 560064, India; rdasheee@gmail.com (R.D.); jyothireddy.kalvakurthi@gmail.com (K.J.R.)
5 School of Electrical Engineering, Vellore Institute of Technology, Vellore 632014, India; g.arunkumar@vit.ac.in
6 Department of Electrical and Computer Engineering, Hawassa University, Hawassa P.O. Box 05, Ethiopia
7 Department of Electrical and Electronics Engineering, Aditya College of Engineering, Surampalem 533437, India; ravieeejntu@gmail.com
* Correspondence: dhanamjayulu.c@vit.ac.in (D.C.); baseemkh@hu.edu.et (B.K.)

Abstract: The deployment of a static synchronous compensator within a microgrid can facilitate voltage and reactive power regulation, leading to enhanced stability and reliability. Within a microgrid setting, the effectiveness of a STATCOM in balancing the power supply is influenced by several factors, including the system configuration, the operating conditions, and the specific requirements of the power grid. The capacity, response time, and magnitude of system disturbances also play a role in determining the STATCOM's ability to balance the power supply. To ensure the successful integration of a STATCOM within a microgrid, coordinating the control system with other distributed energy resources (DER), especially when multiple control strategies are employed, can be a challenging task. Therefore, a meticulously designed control system is indispensable to guarantee the microgrid's efficient and effective operation. The use of GA in LSTM tuning can accelerate the process of identifying the optimal hyperparameters for a specific task, obviating the need for time-consuming and computationally expensive grid searches or manual tuning. This method can be particularly advantageous when handling large data sets and complex models. In this paper, an attempt has been made to model the STATCOM to communicate with the microgrid, tuned using LSTM–GA, for the effective calculation of real and reactive power support during grid disturbances.

Keywords: algorithm; GA; PSO; PSO–LSTM; search space

Citation: Swain, D.; Viswavandya, M.; Dash, R.; Reddy, K.J.; Chittathuru, D.; Gopal, A.; Khan, R.; Ravindra, M. P2P Coordinated Control between SPV and STATCOM in a Microgrid for Power Quality Compensation Using LSTM–Genetic Algorithm. *Sustainability* **2023**, *15*, 10913. https://doi.org/10.3390/su151410913

Academic Editor: Noradin Ghadimi

Received: 13 May 2023
Revised: 3 July 2023
Accepted: 8 July 2023
Published: 12 July 2023

1. Introduction

A microgrid is a type of electrical system that can operate independently or in coordination with the main grid. It consists of one or more distributed energy resources (DERs), such as solar panels, wind turbines, batteries, or generators, which are used to generate or store electricity [1]. Microgrids are designed to provide reliable, efficient, and eco-friendly power to local communities, businesses, and institutions, particularly in remote or off-grid areas where access to the main grid is limited or unreliable. Additionally, they can function as a backup source of power during emergencies, such as grid outages or natural disasters.

Voltage fluctuations are a common power quality issue in microgrids, especially those that incorporate renewable energy sources such as solar and wind. These sources have variable outputs, causing voltage fluctuations that can negatively impact the stability

and performance of the microgrid [2]. Voltage fluctuation can be addressed based on voltage regulation. Voltage regulation is the process of keeping the voltage level in an electrical system stable and constant. This process is particularly important in microgrids, where voltage regulation is critical to ensuring dependable and efficient system operation, especially when intermittent renewable energy sources are present. To ensure voltage regulation in a microgrid, voltage regulators such as automatic voltage regulators (AVRs) or static VAR compensators (SVCs) can be used. These devices can regulate voltage levels in real time by increasing or decreasing the reactive power output of the system.

A static synchronous compensator (STATCOM) is a power electronics device that is frequently used for voltage regulation and reactive power compensation in electrical power systems. It is a type of flexible AC transmission system (FACTS) device that can introduce reactive power into the system to enhance the power quality and voltage stability. With the capacity to supply both capacitive and inductive reactive power, the STATCOM can react quickly to changes in system conditions, making it a versatile device that is appropriate for various applications, including microgrids [3].

Ping He et al. [4], in their paper, present a coordinated control strategy for a PSS and STATCOM, two critical power system devices. The goal of this approach is to enhance power system stability and damping, particularly in the presence of disturbances such as faults or sudden load changes. The study employs a multi-machine power system model and simulation techniques to evaluate the effectiveness of the proposed coordinated control strategy in various scenarios. According to the simulation outcomes, the strategy significantly improves the power system stability and damping and outperforms other control methods that disregard the coordination between the PSS and STATCOM.

Kaliaperumal Rukmani et al. [5] introduce a new approach to optimize the allocation of distribution static compensators (D-STATCOMs) in distribution systems where there is uncertainty. D-STATCOMs are crucial in enhancing the power quality and stability of distribution systems by injecting reactive power. The proposed method involves a combination of fuzzy logic and particle swarm optimization (PSO) algorithms to determine the optimal locations and sizes of D-STATCOMs. Fuzzy logic is utilized to manage uncertainties in the system parameters, while the PSO algorithm is utilized to locate the optimal solution.

Tariq, M. et al. [6], in their article, describe a new approach to voltage regulation and power quality improvement using static synchronous compensators. The proposed method involves adjusting the phase angle between the current and voltage using a simple PI controller to control the output voltage of the STATCOM. The effectiveness of the proposed method is evaluated through simulation studies, which show that it can successfully regulate the voltage and improve the power quality.

Anil Bharadwaj et al. [7] propose a novel approach to tuning PI and PID controllers in power systems equipped with various types of flexible AC transmission system devices, including a STATCOM, SSSC, and UPFC. The proposed method aims to minimize the damping of oscillations in the power system by adjusting the parameters of the controllers. To evaluate the performance of the proposed tuning method, the authors use a multi-machine power system model and conduct simulation studies. The results indicate that the proposed method can effectively improve the damping of oscillations in the power system and outperform other tuning methods that do not consider the presence of FACTS devices.

Sarath Perera et al. [8] present a framework for the reduction of power network oscillations with the use of static synchronous compensators and the synthesis of H2/H∞ controllers. The framework employs an H2/H∞ synthesis technique to design the controller and improve the stability of the power system. The paper evaluates the effectiveness of the proposed framework through simulations using a power system model with a STATCOM, and the results indicate that the framework can effectively reduce oscillations in the power system and enhance its stability.

Claudia Battistelli et al. [9] suggest using the whale optimization algorithm (WOA) to develop power system stabilizers for multi-machine power systems. The goal of this method is to enhance the stability of the system by designing power system stabilizers that

minimize oscillations. The authors evaluate the proposed method by simulating it using a multi-machine power system model, and the findings show that the WOA-based stabilizers can effectively damp oscillations in the power system and enhance its stability [7].

Liangce He et al. [10] propose a method to optimize the economic and environmental performance of an integrated regional energy system by incorporating an integrated demand response into the environmental economic dispatch process. The proposed method optimizes the dispatch of different energy sources to minimize the total cost and emissions of the system while considering the impact of DR on the load demand. The effectiveness of the proposed method is evaluated through simulations, which show that it can effectively reduce the total cost and emissions of the system while considering the impact of DR.

D. Ranamuka et al. [11,12] propose a strategy for the control of the power flow in distribution systems using the coordinated control of distributed solar–PV and battery energy storage units. The objective is to enhance the stability and efficiency of the distribution systems through real-time power flow control via distributed energy resources. The proposed method is evaluated using a distribution system model with solar–PV and battery energy storage units, and the simulation results demonstrate its effectiveness in improving the stability and efficiency of the distribution system [13,14].

The paper [15,16] proposes a power system stabilizer (PSS) design for the damping of low-frequency oscillations in a multi-machine power system with the integration of renewable power generation. The proposed PSS design is based on eigenvalue analysis and aims to optimize the damping of low-frequency oscillations in the system. To evaluate the effectiveness of the proposed PSS design, simulations are conducted using a multi-machine power system model with renewable power generation. The simulation results indicate that the proposed PSS design can effectively dampen low-frequency oscillations and enhance the stability of the power system [17,18]. As observed in the literature review, GA searches for a solution in the space based on probabilistic principles. Therefore, there is no sufficient guarantee that the system will always be optimized to the global optimal solution. Depending on the complexity of the STATCOM control problem and the specific fitness function used, there is a risk that GA may become trapped in local optima and fail to discover the best possible controller settings.

The performance of particle swarm optimization (PSO) in controlling STATCOMs in power systems may be limited by multiple factors [19,20]. One of these factors is the high sensitivity of the PSO algorithm to the initial conditions, which may lead to suboptimal solutions or becoming stuck in local optima. A solution to this problem can be achieved by starting with a good initial population and modifying the parameters of the PSO algorithm [21,22]. Another limitation is the inability of the PSO STATCOM to handle uncertainties in the power system, such as variations in renewable energy sources or changes in load demand. This may result in suboptimal STATCOM operation and reduced performance in controlling the power system [23,24].

Hyperparameter selection in the case of optimization is a critical challenge as it is the hyperparameters that will determine the area of optimization. Overfitting is a common problem in the case of data fitting, which is primarily due to the involvement of long-term dependencies. To avoid such conditions, it is necessary to store past data in the system's memory for the easy analysis and prediction of situations under abnormal conditions.

PSO, inspired by swarm behavior, is a population-based optimization algorithm that seeks optimal solutions in a problem space. In contrast, long short-term memory (LSTM) is a type of recurrent neural network (RNN) renowned for capturing and learning temporal dependencies in sequential data. The integration of PSO with LSTM involves utilizing PSO as a training algorithm to optimize LSTM's weights and biases. PSO achieves this by iteratively updating the particle positions and velocities based on personal and global best solutions, enabling LSTM to discover optimal parameter values for enhanced predictive accuracy. However, empirical studies consistently demonstrate LSTM's superiority over PSO-based LSTM models. LSTM's inherent capability to capture long-term dependencies and handle sequential data empowers it in time series prediction tasks. LSTM exhibits

stronger learning capabilities and generalization power compared to PSO, which primarily focuses on optimization.

The combination of LSTM and genetic algorithm (GA) can have diverse applications, including time-series prediction, anomaly detection, and optimization problems [25,26]. For time-series prediction, LSTM can be utilized to forecast future values based on historical data, while GA can be used to optimize the hyperparameters of the LSTM model, such as the learning rate and the number of LSTM cells. In anomaly detection, LSTM can learn the regular patterns in data and identify any deviations from them, and GA can optimize the threshold for the detection of anomalies [27,28]. In optimization problems, LSTM can serve as a surrogate model for the evaluation of the objective function, and GA can search for the optimal solution.

In this paper, an attempt has been made to design a STATCOM, particularly in a microgrid, to provide voltage and reactive power support under variations in environmental parameters. We have analyzed various grid disturbances related to the injected current, voltage, and harmonics when utilizing a STATCOM. These disturbances include voltage sags and swells, which are temporary voltage decreases or increases caused by faults or abrupt changes in load demand. The current injected by the STATCOM is carefully examined to address and stabilize the voltage levels during such disturbances. Furthermore, we investigate the impact of harmonics on the grid, which refer to additional frequencies that can distort the sinusoidal waveform of the power supply. Through an evaluation of the harmonic content within the injected voltage, the effectiveness of the STATCOM in mitigating harmonic distortion and enhancing the power quality is assessed. By considering these grid disturbances, the study provides valuable insights into the STATCOM's performance and capabilities in effectively managing voltage fluctuations and harmonics, thus ensuring a reliable and efficient power supply. LSTM has been used to store the previous memory and historical data of the power quality issues and the amount of reactive power support, whereas genetic algorithm provides support for hyperparameter optimization. The objectives of the research can be summarized as follows.

- Design of LSTM–GA mathematical modeling for STATCOM microgrid analysis. The limitation of GA modeling in handling convex optimization can be best addressed using this LSTM–GA model. LSTM will provide memory-level access to the past historical data along with the lookup table.
- Modeling of the proposed system using MATLAB Simulink model and its validation under dynamic non-linear loading conditions and PV output variation with respect to environmental parameters.
- A detailed comparative analysis with another established benchmarking model in terms of stability analysis; validation has been carried out with a step function.

2. STATCOM Architecture and Analysis

STATCOMs play a vital role in power systems by regulating the voltage and providing reactive power support. These devices are built on a voltage source converter (VSC) architecture and are connected to the grid through phase reactors and a step-up transformer. The VSC incorporates insulated gate bipolar transistors (IGBTs) in a modular multi-level converter (MMC) configuration.

The primary objective of a STATCOM is to control the voltage at its point of connection to the grid. It achieves this by generating or absorbing reactive power, effectively regulating the system voltage and enhancing power system stability. Unlike conventional reactive power compensation devices, such as capacitor banks or synchronous condensers, STATCOMs offer the advantages of a rapid response and continuous control across a wide range of operating conditions.

At the core of a STATCOM lies the VSC, comprising power semiconductor switches, particularly IGBTs, which can swiftly switch on and off to produce the desired voltage waveform. The MMC configuration within the VSC allows for high-voltage operation and facilitates the generation of a high-quality voltage with minimal harmonic distortion. By

converting DC power into AC power, the VSC allows the STATCOM to inject or absorb reactive power into the grid as required.

Through the dynamic adjustment of the voltage waveform produced by the VSC, the STATCOM actively regulates the grid voltage, compensates for reactive power imbalances, mitigates voltage flicker, improves the power factor, and bolsters the overall power system stability and reliability. The control system of the STATCOM continuously monitors the system conditions and employs feedback control algorithms to adapt the voltage output of the VSC accordingly. The presence of a step-up transformer enables the STATCOM to connect to the high-voltage transmission grid, ensuring appropriate voltage levels for effective power transmission and distribution. Additionally, the phase reactors provide impedance and protection to the STATCOM system while limiting the flow of short-circuit currents.

The diagram in Figure 1 illustrates the principle behind the controlled switching of the IGBT valves in a single sub-module, which generates the fundamental three-level waveform utilized by the STATCOM to control the contribution of reactive power to the grid. However, the performance, rating, and controllability of the STATCOM can be significantly enhanced by the connection of multiple sub-modules in series.

When these sub-modules are interconnected, it enables the construction of a voltage waveform with an improved resolution. This means that the voltage can be precisely controlled with finer granularity, resulting in the more accurate regulation of the reactive power. The increased resolution enhances the overall performance of STATCOM, enabling it to provide more efficient and precise control over reactive power compensation in the grid. Figure 2 presents the STATCOM vector analysis under the stand-by, inductive, and capacitive modes, respectively.

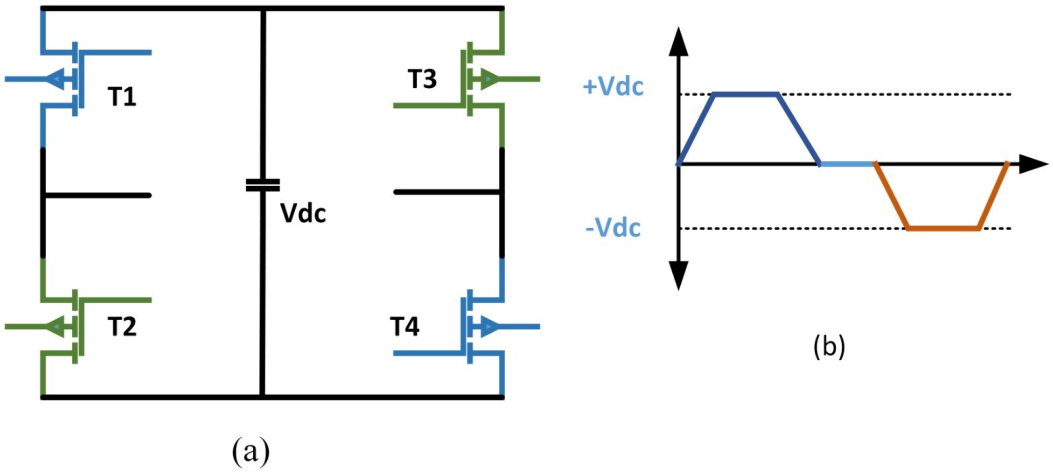

Figure 1. STATCOM. (**a**) Typical full-bridge sub-module, (**b**) output waveform.

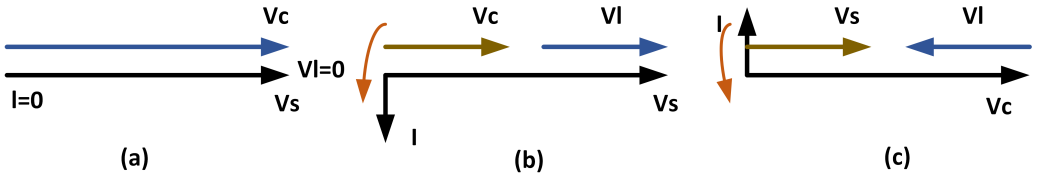

Figure 2. STATCOM. (**a**) Standby mode, (**b**) inductive mode, (**c**) capacitive mode.

Furthermore, the series connection of multiple sub-modules allows for the higher rating capability of the STATCOM. By combining the voltage outputs of each sub-module, the overall voltage level and capacity of the STATCOM can be increased. This expanded rating capability enables the STATCOM to handle larger reactive power demands and provide enhanced support to the power system (Figure 3).

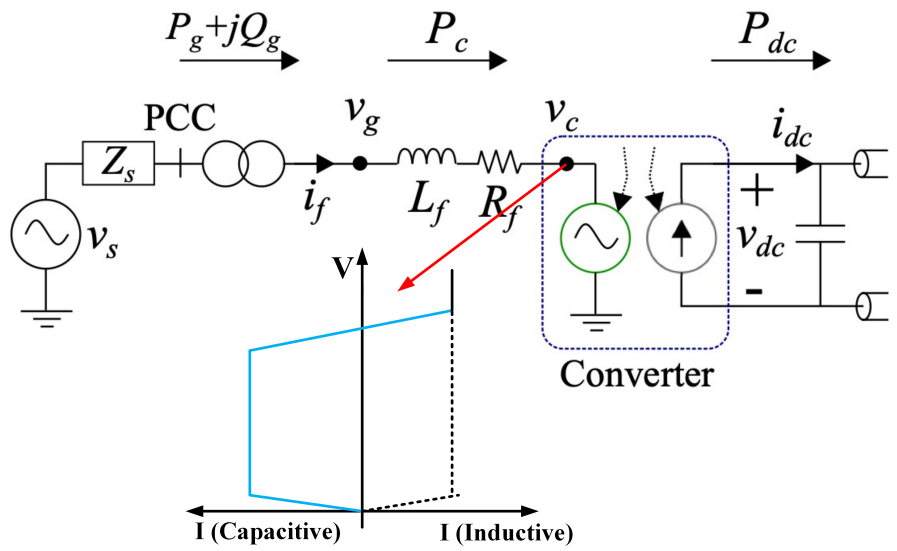

Figure 3. STATCOM along with IV characteristics [8].

Two control loops are generally involved in a VSC-based STATCOM architecture. The outer control loop will control the V_{ac} or V_{dc} depending on the control requirements and the number of variables involved in the system. The inner control loop controls the actual response with the set values. Therefore, the current control loop becomes

$$V_c^d = \omega_g L_f i_f^g - (K_p - \frac{K_i}{s})(i_f^{d*} - i_f^d) + V_g^d \quad (1)$$

$$V_c^q = -\omega_g L_f i_f^g - (K_p - \frac{K_i}{s})(i_f^{q*} - i_f^q) + V_g^q \quad (2)$$

Equations (1) and (2) represent the direct and quadrature axis control of the voltage waveform in the inner current control loop.

3. Problem Formulation and Solution Methodology

The single-line multi-machine bus (SIMB) microgrid implementing a STATCOM is shown in Figure 4.

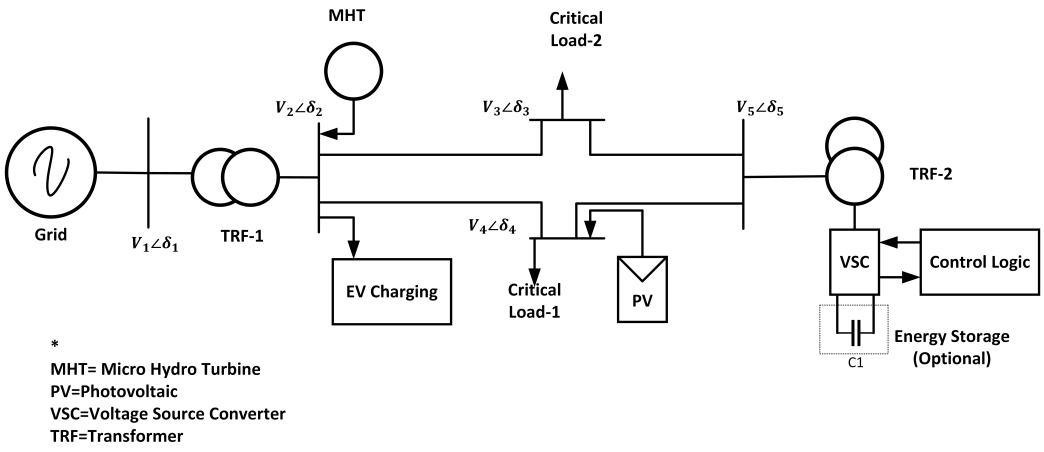

Figure 4. SIMB architecture for microgrid.

This architecture is widely used for STATCOM performance evaluation under the microgrid model. The model mainly consists of an infinite bus connected to a synchronous generator at one side through a two-winding transformer; at the other side, it is connected to a microgrid architecture supported by a STATCOM and PV source. The STATCOM under

investigation is a GTO-based voltage source converter (VSC). Here, the VSC will generate a controllable voltage in accordance with leakage reactance. Then, the voltage difference between the STATCOM terminal and bus will determine the type of power exchange, such as active power or reactive power, between the two devices. The amount of reactive power exchange can be controlled using the voltage and phase angle δ.

Therefore, the nonlinear equation between the STATCOM's voltage and current becomes

$$I_{LO}^{*} = I_{Load} + jI_{Loq} \tag{3}$$

and

$$V_0 = CV_{dc}(cos\theta + jSin\theta) \tag{4}$$

In Equation (3), I_{LO}, I_{Load} and I_{Loq} represent the STATCOM's load current and the load current with respect to the d-axis and q-axis, respectively. Similarly, V_{dc} represents DC-ref voltage at the input of the STATCOM. Further, Equation (4) can be modified as follows:

$$V_0 = \frac{C^2}{C_{dc}} V_{dc} \angle\theta [I_{Load} Cos\theta + I_{loq} Sin\theta] \tag{5}$$

Equation (5) represents the output voltage equation of the STATCOM, designed based on the d- and q-axis current levels. Here, "c" represents the ratio between the AC and DC voltages. In order to calculate the virtual electrical torque, the speed deviation has been taken into consideration, $\delta\omega$. Therefore, the new damping controller can be designed as a lead–lag compensating controller.

Based on Equation (5), it is understood that the proper tuning of the STATCOM parameters, such as θ and C, is required to minimize the damping at the injected voltage level. Therefore, the optimization objective function can be formulated as

$$J = \Sigma_{i=1}^{N_p} \int_0^t |\delta\omega_i| t dt \tag{6}$$

In Equation (6), t represents the simulation time for the model and N_p represents the size of the population in genetic algorithm. The objective is to minimize the cost function and thereby improve the settling time and overshoot.

During cost function optimization using GA, there is a state called the fitness function or value evaluation, which requires a probability evaluation of each chromosome pair in the objective function. This requires an iteration to be run in order to evaluate the fitness value. Therefore, in order to reduce the optimization time in evaluating the constraints at each step, long short-term memory (LSTM) has been introduced. LSTM will hold the best solution for subsequent levels of iteration and thereby reduce the optimization time by t_{n-best}, where t_n is the total duration of the iteration, which has been reduced to t_{n-best} based on the best solution.

Figure 5 shows the LSTM–GA architecture for STATCOM PI controller optimization. As observed, GA produces two sets of optimized data related to the electrical torque reference value and C value, which is simply the ratio of the DC injected voltage to the AC injected voltage. The LSTM encoder will hold the best-optimized value during GA iteration, along with the time stamp. Therefore, during the decoding process, the same time stamp can be utilized for reactive power generation and subsequent voltage support, along with SSR damping.

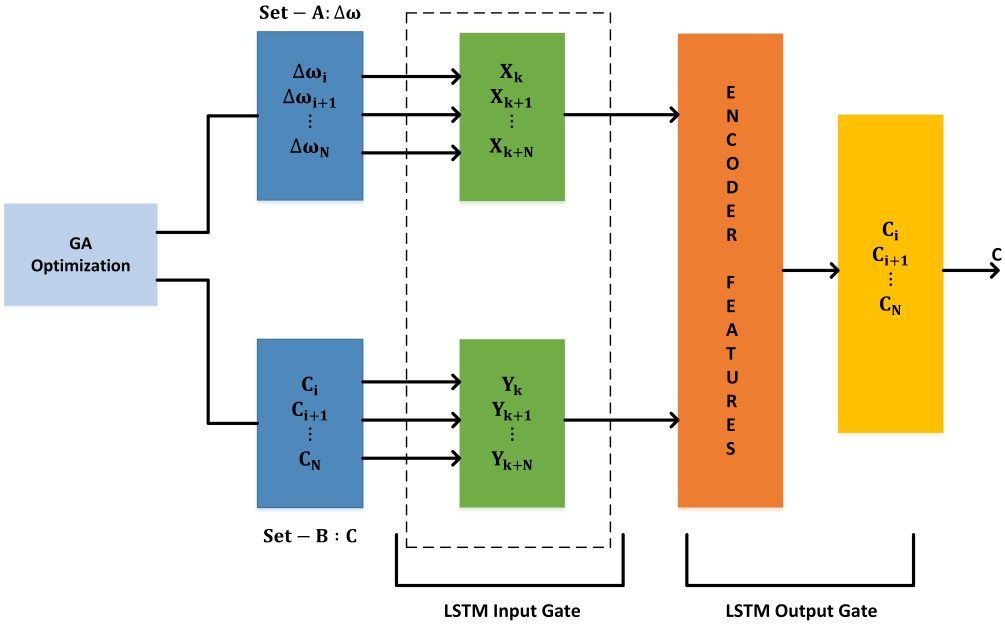

Figure 5. LSTM–GA architecture for STATCOM PI controller optimization.

In order to properly train the model, it is highly recommended to activate each layer in the LSTM architecture using the appropriate activation function. The inputs to the activation layer are represented by f and V, while the output of the LSTM network provides the reactive power compensation factor in $V\angle\delta$. Generally, each layer in the activation module evaluates the weighted sum of all its input connections and maps it to an output, as shown in Equation (7), where λ represents the layer of the input module.

$$V_{\lambda_j} = \sum_i V\angle\delta_{\lambda_{ji}}\, y_i \quad for\ \ \lambda \in \{f, V, Q, P\} \tag{7}$$

The recurrent connection between each layer λ can be varied by changing the unit of i. By applying the squashing function $f_{\lambda i}$ on y_i, the output for each layer λ can be modeled as

$$y_{\lambda_j} = f_{\lambda i}(V_{\lambda j}) \quad for\ \ \lambda \in \{f, V, Q\} \tag{8}$$

In Equation (6), a cascaded inner current control loop has been implemented to interconnect LSTM and GA with the PI control features. Each memory cell unit in LSTM holds the previous state in the same proportion as the activation in the forget layer gate. Therefore, the current state vector S_{cj} updates itself based on the modulus of the activation function at the input gate. Hence,

$$S_{cj} = Y_{\psi j}\hat{S_{cj}} + y_{ij}x_{cj} \tag{9}$$

Based on Equation (9), the learning rate can be made more effective by designing each layer to track the activity flow over time. To achieve this, an eligibility trace module has been provided to trace the most recent activity value, as presented in Equation (8).

$$\sum \lambda_{ji} = Y_i \ldots\ldots \forall\lambda \in [v\angle\delta, \theta] \tag{10}$$

Similarly, the memory cell and forget gate can be modeled as

$$\sum P_{ji} = Y_{\epsilon i}\hat{e}P_{ji} + Y_{lj}Yi \tag{11}$$

To develop a robust algorithm to track the required output against the predicted output, a time range of [0, 1] has been implemented. The cross-entropy function has been used to quantify the error between the predicted and actual outputs of the LSTM module. The pseudo-code for the implementable algorithm is presented in Algorithm 1.

GA requires the appropriate encoding and representation of solutions as chromosomes. In convex optimization (Algorithm 1), the solutions are typically represented as vectors or matrices, and the optimization algorithms exploit the convex structure. The mapping of these representations to the chromosome structure is used in GA.

Algorithm 1 Voltage and angle error evaluation—training pseudo-code

Require: V_{er},I_{der}, θ_s
Ensure: 3 Variable state transition pattern
  for $V_t = 1$ **do**
    for `f=-1` **do**
      for $V_{er} = 0$ **do**
        `Evaluate` V_{er} `and` θ_s
      end for
    end for
  end for
  Weight w_i=min(δT_{er}, δW_{er},θ_s)
  $\theta_x V_x$ = max($\theta_{x-1} V_{x-1}$, $\theta_x V_x$)
  if $(M_{L-1}^{t_0} - M_L^{t_1}) \leq 0.02$ **then**
    break
  else
    $(M_{L-1}^{t_0} - M_L^{t_1}) \leq 0.02$
  end if

4. Result Analysis

The proposed LSTM–GA model has been designed using MATLAB Simulink as per the architecture shown in Figure 6.

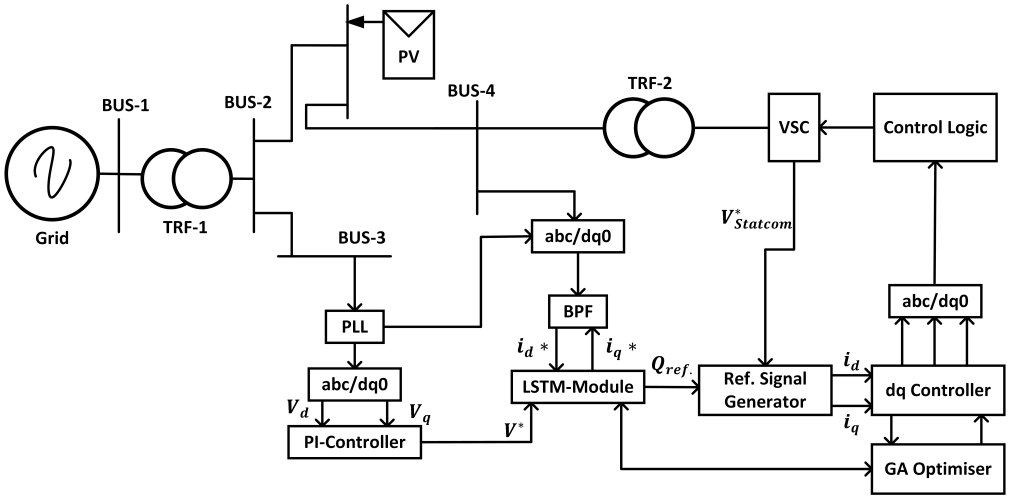

Figure 6. Simulink model for STATCOM microgrid coordinated control action using LSTM and GA.

Here, the LSTM module will process the i_d, i_q, and v^* values to determine the required amount of reactive power for the grid, which the STATCOM needs to produce. LSTM will share the hyperplane with the GA-optimized module to evaluate the agent position and initialize the chromosome parameter with four different variables.

Table 1 shows the STATCOM model's parameters, which have been used in the Simulink model to perform the analysis. All the set points, especially the AC voltage reference magnitude and DC voltage set point, are assumed to be per unit. All the AC and DC regulator gains have been evaluated based on a genetic algorithm ensemble with the classical Ziegler–Nicholas method.

Table 1. STATCOM module parameters for Simulink model used in microgrid architecture.

Sr. No.	Name of Parameter	Rating	Remarks
1	Coupling capacitor	420 micro F	Storage
2	PWM frequency	2.33 kHz	Under Modulation
3	Coupling TFR	210:800	Centre Tap
4	AC ref. voltage	1 pu	707 V
5	DC ref. voltage	750 V	-
6	AC voltage regulator gain	[0.52 0.39]	ZNM
7	DC voltage regulator gain	[0.03 0.27]	ZNM-GA
8	Current regulator gain	[0.11 0.17]	GA-LSTM

As observed, the regulator gain for the AC voltage is [0.52 0.39], which was evaluated through the Ziegler–Nicholas method (ZNM), and the corresponding DC voltage gain was evaluated through ZNM and GA. Moreover, the current regulator gain, which is a function of both the AC voltage and DC voltage regulation gains, has been evaluated through the ZNM–LSTM ensemble with GA. Thus, a single hyperplane can be maintained throughout the analysis.

Figures 7 and 8 present the LSTM–GA performance analysis for two different values of μ, i.e., 0.11 and 0.18, respectively. As observed, the objective of LSTM–GA is to forecast the required reactive power support for the microgrid, which is 15.58% and 12.10%, respectively, in this case. With the increase in the chromosome size, the system is able to accurately predict the amount of required reactive power support for the grid. In the subsequent discussion, the performance analysis has been carried out with μ of 0.18.

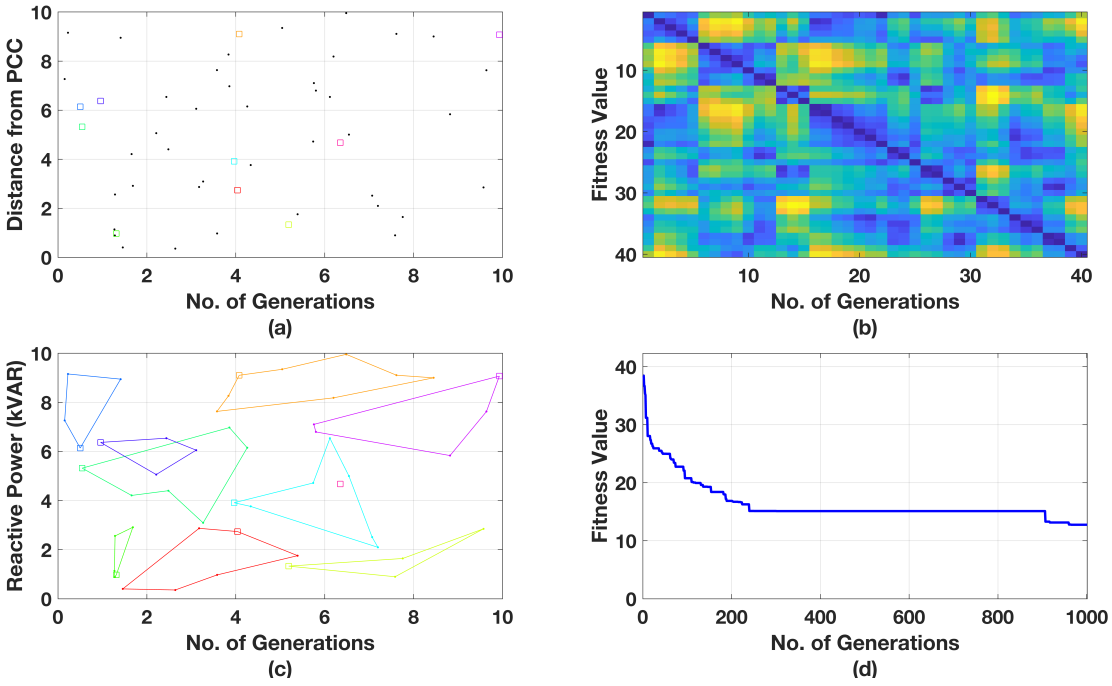

Figure 7. GA performance with $\mu = 0.11$. (**a**) FACTS location initialization, (**b**) reactive power support range, (**c**) percentage of reactive power support, (**d**) best solution history.

Figure 9 presents the STATCOM DC link voltage for three different models (a) the Fuzzy–PI STATCOM, (b) PSO–PI STATCOM, and (c) proposed LSTM–GA–PI STATCOM (LGPS). As observed, the "LGPS" model produces a standard optimized DC link voltage of 700.24 V (Figure 9c), which is 0.32% less compared to the fuzzy model (Figure 9a) and 0.23% less compared to the PSO STATCOM (Figure 9b) model. This reduction in the voltage percentage will also reduce the voltage stress on the switch.

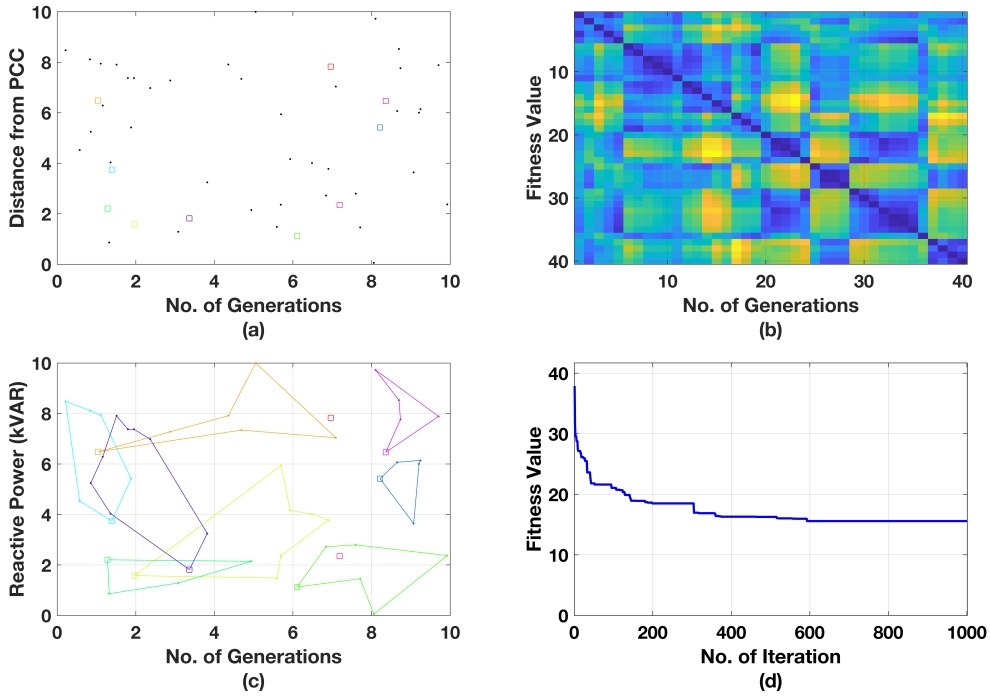

Figure 8. GA performance with $\mu = 0.18$. (**a**) FACTS location initialization, (**b**) reactive power support range, (**c**) percentage of reactive power support, (**d**) best solution history.

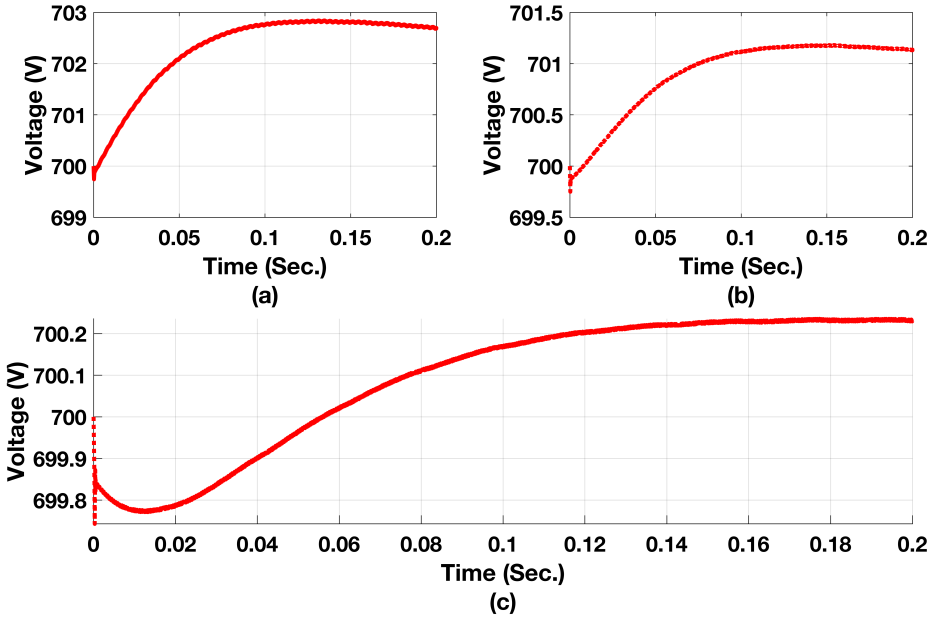

Figure 9. STATCOM DC link voltage obtained from microgrid side. (**a**) Fuzzy PI Controller (**b**) PSO-PI Controller (**c**) LSTM-GA-PI controller.

Figure 10 presents the STATCOM DC link current for all the models. Here, it is observed that with the Fuzzy STATCOM model, the system exhibits sub-synchronous resonance (SSR) between 0.002 and 0.005 s, and a similar SSR was also noticed with the PSO STATCOM, from 0.006 to 0.008 s. However, an SSR limit of 2.8% was noticed with the hyperplane concept using LSTM and GA. As compared to the Fuzzy and PSO STATCOM models, the SSR has been reduced by 7.2% and 9.43% with the proposed "LGPS" model. The SSR also reduces the voltage swell at the point of common coupling and thereby indirectly supplies the reactive power compensation in the line.

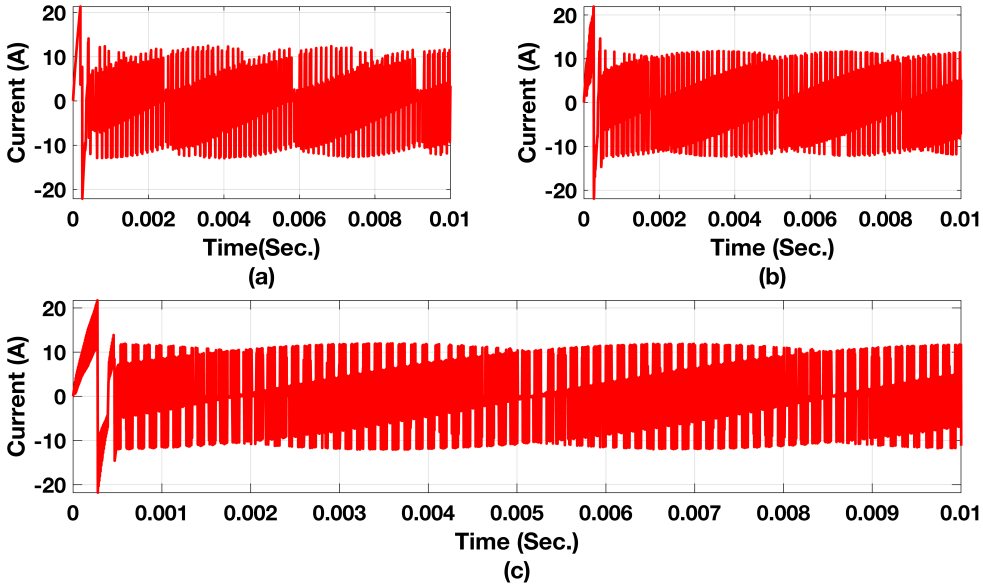

Figure 10. STATCOM DC link current obtained from microgrid side. (**a**) Fuzzy–PI STATCOM, (**b**) PSO–PI STATCOM, and (**c**) LGPS.

Figure 11 presents the STATCOM injected current and Figure 12 presents the STATCOM injected voltage at the point of common coupling. As observed, the injected current using the proposed model is 11.23 Amp. Similarly, a voltage level of 188 V has been maintained at the PCC, against 200 V and 197 V in the case of the fuzzy and PSO-enabled PI controllers. The THD levels of all three models for the injected current are shown in Figure 13. With the proposed model, the THD has been reduced to 11.44%, against 15.04% in Fuzzy–PI STATCOM and 12.39% in PSO–PI STATCOM.

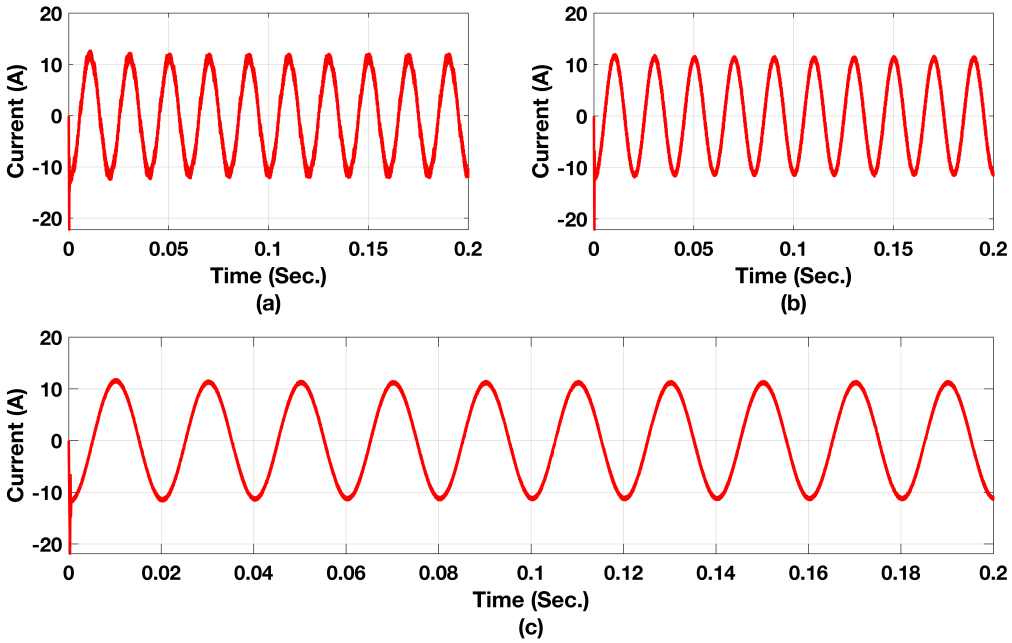

Figure 11. STATCOM injected current at PCC into microgrid. (**a**) Fuzzy–PI STATCOM, (**b**) PSO–PI STATCOM, and (**c**) LGPS.

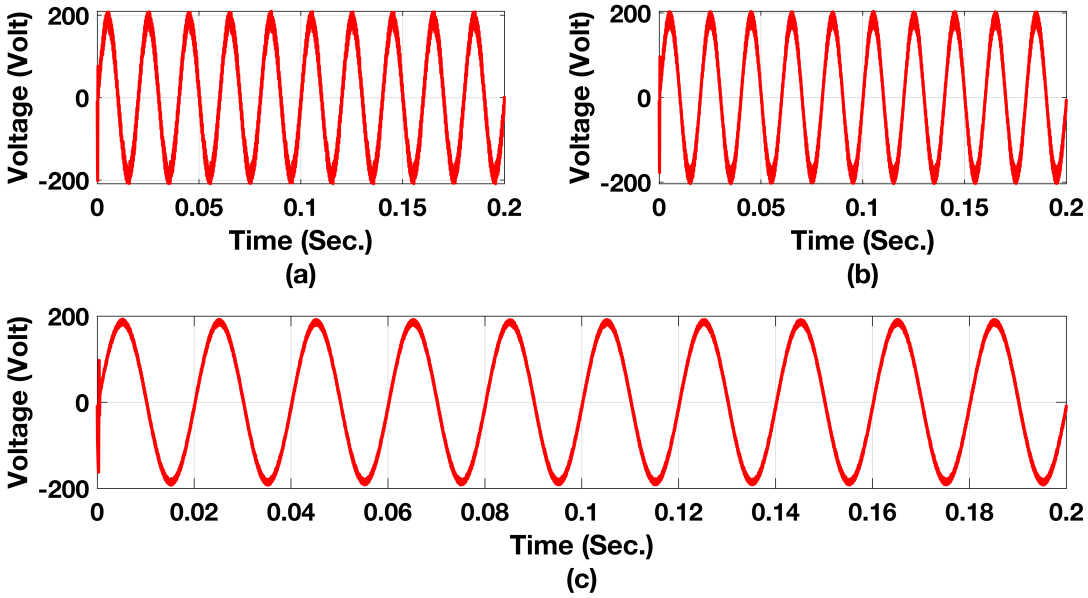

Figure 12. STATCOM injected voltage at PCC into microgrid. (**a**) Fuzzy–PI STATCOM, (**b**) PSO–PI STATCOM, and (**c**) LGPS.

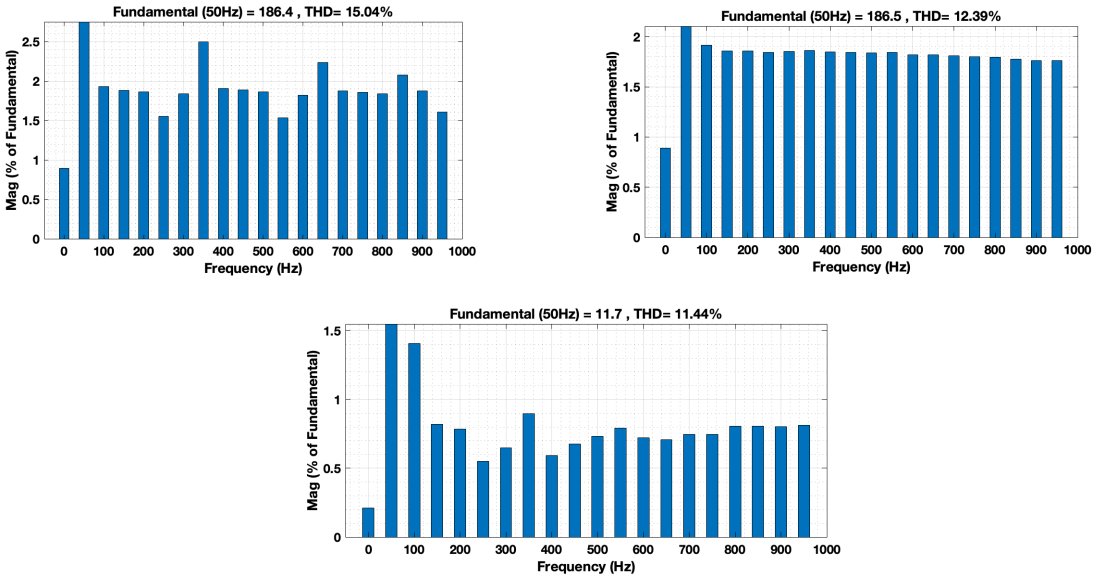

Figure 13. Total harmonic distortion of current waveform at the terminal of PCC.

Figure 14 presents the voltage waveform of the r-phase of the microgrid. In Figure 14a, it is observed that the voltage is 252 V with harmonic content of 12.3% and that of for Figure 14b, PSO-PI controller, the voltage becomes 238 V with harmonic content of 10.78%. However, with proposed controller Figure 14c the voltage is maintained at 231.7 V. The percentage of harmonics injected by the STATCOM becomes 18% and that in the proposed model becomes 12.03%.

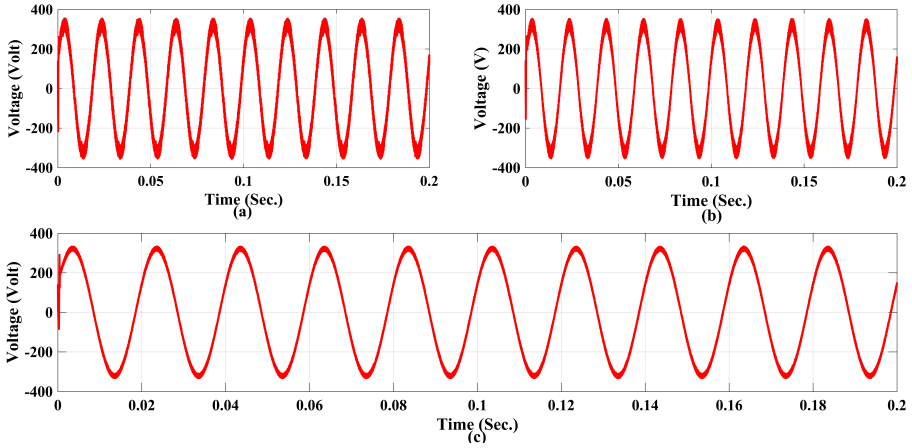

Figure 14. Voltage waveform of r-phase of microgrid. (**a**) Fuzzy PI Controller (**b**) PSO-PI Controller (**c**) LSTM-GA-PI controller.

5. Discussion

The P2P coordinated control between the SPV and STATCOM in a microgrid for power quality compensation using LSTM–genetic algorithm has been analyzed experimentally (MATLAB simulation) with two benchmarking models, the Fuzzy–PI and PSO–PI models. On analyzing the model, the observations are as follows.

Table 2 shows the power quality analysis of the STATCOM microgrid. It is observed that maximum harmonics have been produced with the Fuzzy–PI STATCOM of the order of 15.43%, and the least harmonics produced amount to 11.22%, with the proposed model. In all three cases, the broad band has been maintained for the notch. As compared to all the other algorithms, with the LSTEM–GA–PI STATCOM, the lowest DC offset was observed. Similarly, Table 3 presents the time-domain analysis of the STATCOM–PI controller. By testing these different control algorithms against a step function input, the time-domain analysis allowed for a comparison of their performance in terms of how well they respond to sudden changes and achieve the desired system behavior. The proposed algorithm produces 8.84% of overshoot, which is also the lowest among all the benchmarking models.

Table 2. Power quality analysis of STATCOM microgrid.

Sr. No.	Technique	Power Quality Attribute	Magnitude
01	Fuzzy–PI STATCOM	DC Offset	0.21%
		Harmonic Current	15.34%
		Inter Harmonics	1.87%
		Notching	Broad Band
		Noise	0.82%
02	PSO–PI STATCOM	DC Offset	0.14%
		Harmonic Current	12.72%
		Inter Harmonics	1.25%
		Notching	Broad Band
		Noise	0.57%
03	LSTM–GA–PI STATCOM	DC Offset	0.07%
		Harmonic Current	11.22%
		Inter Harmonics	0.87%
		Notching	Broad Band
		Noise	0.44%

Table 3. Time-domain analysis of STATCOM–PI controller.

Sr. No.	Technique	Parameters	Magnitude	Remarks
01	Fuzzy–PI STATCOM	Delay Time Rise Time Peak Time Settling Time Max. Overshoot	0.58 0.62 0.77 2.23 14.44%	Marginally Stable Critically Damped
02	PSO–PI STATCOM	Delay Time Rise Time Peak Time Settling Time Max. Overshoot	0.49 0.53 0.65 1.90 12.27%	Asymptotically Stable Critically Damped
03	LSTM–GA–PI STATCOM	Delay Time Rise Time Peak Time Settling Time Max. Overshoot	0.35 0.38 0.47 1.36 8.84%	Stable

Figure 15 presents the voltage and current performance of the STATCOM at the PCC. Figure 15a presents the voltage and current waveform for the Fuzzy–PI STATCOM. As observed, the current has undergone oscillations from 0.3 s to 0.4 s. This is due to the unavailability of internal memory and also the inability of the controller to dynamically assign the reference voltage for the grid-side converter of the DFIG. Similarly, for the PSO–PI controller, the oscillations are less as compared to the GA–PI controller, as presented in Figure 15b. However, with the proposed LSTM–GA–PI STATCOM (Figure 15c), the oscillations have been damped out completely. This is because of the presence of a memory unit in the feedback loop. The maximum peak overshoot in the current waveform is 0.58 pu, as compared to 0.98 pu and 0.77pu in the Fuzzy–PI and PSO–PI controllers, respectively.

Figure 16 shows the DC offset voltage analysis for the Fuzzy–PI, PSO–PI, and LSTM–GA–PI STATCOM controllers. As observed, the initial oscillation presents negative slope characteristics for LSTM–GA–PI as compared to the other controllers. Similarly, the second transition event from 0.2 s to 0.3 s shows fewer oscillations for the DC offset.

Figure 17 presents the power quality analysis of the STATCOM's injected real and reactive power for the Fuzzy–PI, PSO–PI, and LSTM–GA–PI STATCOMs. As observed in Figure 17a, the reactive power has been absorbed by the STATCOM for three cycles, whereas, for the PSO–PI controller in Figure 17b, it shows oscillations with a time-varying negative slope. However, with the LSTM–GA–PI controller, the reactive power has been injected at 25% so as to reduce the burden on the DFIG stator.

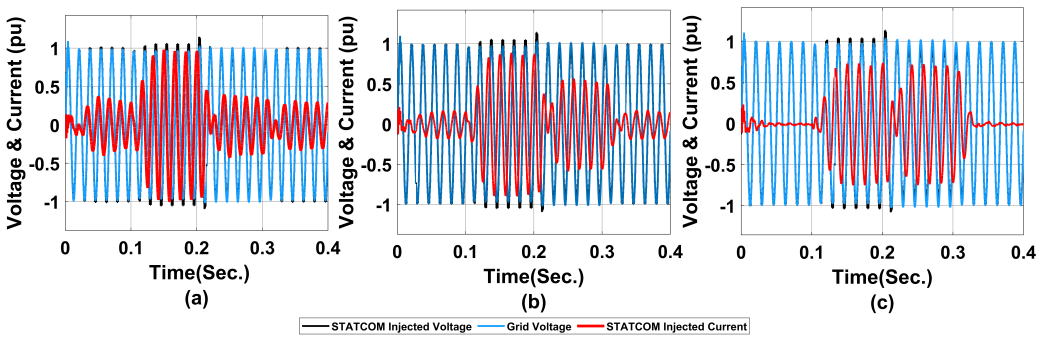

Figure 15. STATCOM performance. (**a**) Fuzzy–PI STATCOM, (**b**) PSO–PI STATCOM, (**c**) LSTM–GA–PI STATCOM.

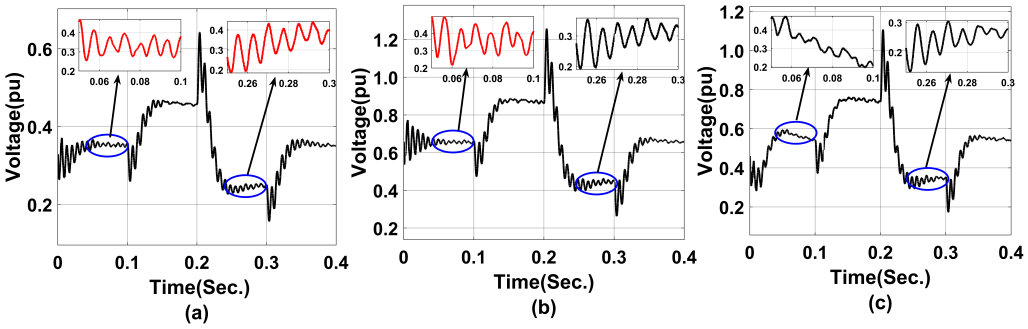

Figure 16. DC offset voltage analysis for DFIG controller. (**a**) Fuzzy–PI, (**b**) PSO–PI, (**c**) LSTM–GA-PI.

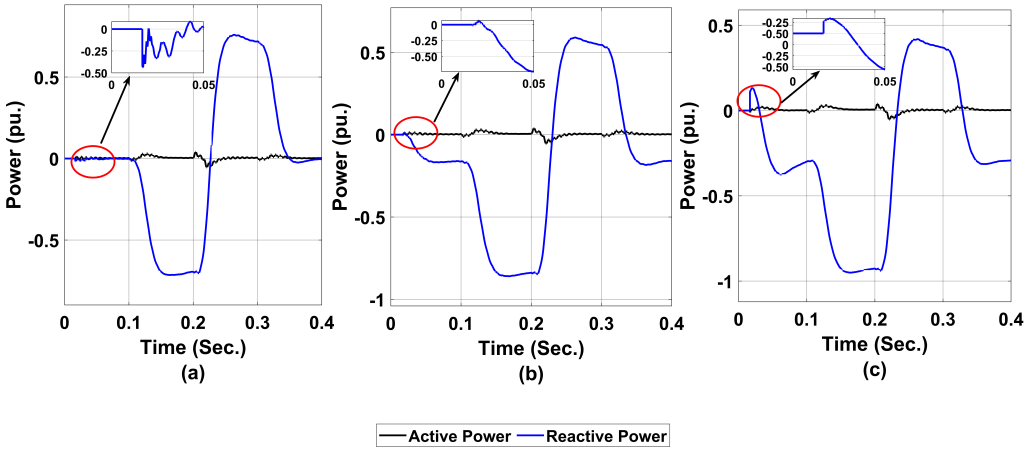

Figure 17. Power quality analysis of STATCOM injected real and reactive power. (**a**) Fuzzy–PI, (**b**) PSO–PI, (**c**) LSTM–GA–PI.

The integration of solar photovoltaic systems in a microgrid represents the utilization of clean and renewable energy sources. This reduces the reliance on fossil fuels and conventional power generation, resulting in lower greenhouse gas emissions and promoting environmental sustainability. A microgrid is a localized and decentralized energy system that can operate independently or in conjunction with the main power grid. Coordinated control between the SPV and STATCOM enhances the microgrid's power quality by ensuring stable voltage and frequency levels. This improved power quality enables the efficient operation of connected devices, minimizes electrical disturbances, optimizes energy consumption, and reduces waste, contributing to sustainability.

The utilization of advanced control techniques, such as LSTM and genetic algorithm, underscores the intelligence of the control system. By leveraging machine learning and optimization algorithms, such as LSTM and genetic algorithm, respectively, the microgrid can adapt to changing conditions, optimize the energy flow, and minimize losses. This intelligent control approach enhances the overall performance and energy efficiency of the microgrid, maximizing the utilization of the available renewable energy resources and contributing to sustainability.

Microgrids are designed to operate autonomously during grid disruptions and enhance the resilience against natural disasters and other disturbances. By incorporating coordinated control between the SPV and STATCOM, the microgrid effectively compensates for power quality issues and maintains a stable energy supply. This increased energy independence improves the microgrid's resilience and reduces the reliance on the main power grid. Ultimately, it contributes to the overall sustainability of the energy system by ensuring a reliable and uninterrupted power supply, particularly during critical situations.

6. Conclusions

The optimal and coordinated performance of a STATCOM and microgrid using LSTM–genetic algorithm has been evaluated in this article using simulation methods under normal and abnormal operating conditions. Both the AC and DC voltage gains of the STATCOM were optimized using LSTM–GA. It was observed that when carefully tuning the parameters, the DC offset for the LSTM–GA STATCOM was reduced significantly to 0.07%, compared to 0.21%, and it also avoids SSR to an extent of 17%.

The harmonic and inter-harmonic components using the LSTM–GA methodology reduce the burden on the transmission line and thereby reduce the overheating of the conductor in a microgrid system under load variation conditions. In order to maintain a proper system balance with respect to the IEC and IEEE standards, the notching level of the broad band range has been maintained. During time-domain analysis, the proposed LSTM–PI–GA model shows a shorter settling time as compared to the other two benchmarking models under the step-changing mode of operation.

The optimized STATCOM device has been presented as a dependable solution to improve the stability of microgrid systems, regardless of whether they are functioning normally or abnormally. This device is capable of suppressing transient oscillations in power and frequency while managing voltage fluctuations caused by external disturbances or changes in load demand. Overall, the STATCOM is a highly effective resource in ensuring the consistent and stable performance of microgrid systems.

Author Contributions: Conceptualization, D.S.; Methodology, D.S.; Software, D.S. and K.J.R.; Validation, M.V., K.J.R., A.G. and M.R.; Formal analysis, D.S., M.V., R.D., K.J.R., A.G., B.K. and M.R.; Investigation, D.S., M.V., R.D., K.J.R. and D.C.; Resources, K.J.R., D.C., A.G., B.K. and M.R.; Data curation, D.S., M.V., R.D., K.J.R., A.G. and B.K.; Writing—original draft, D.S., R.D., D.C. and B.K.; Writing—review & editing, D.S., M.V., R.D., K.J.R., D.C. and M.R.; Visualization, D.C., A.G. and B.K.; Supervision, D.C.; Project administration, D.C.; Funding acquisition, B.K. All authors have read and agreed to the published version of the manuscript.

Funding: This research received no external funding.

Institutional Review Board Statement: Not applicable.

Informed Consent Statement: Not applicable.

Data Availability Statement: Data will be available on request.

Conflicts of Interest: The authors declare no conflict of interest.

References

1. Pullins, S. Why microgrids are becoming an important part of the energy infrastructure. *Electr. J.* **2019**, *32*, 17–21. [CrossRef]
2. Eid, B.M.; Rahim, N.A.; Selvaraj, J.; El Khateb, A.H. Control Methods and Objectives for Electronically Coupled Distributed Energy Resources in Microgrids: A Review. *IEEE Syst. J.* **2016**, *10*, 446–458. [CrossRef]
3. Cagnano, A.; De Tuglie, E.; Mancarella, P. Microgrids: Overview and guidelines for practical implementations and operation. *Appl. Energy* **2019**, *258*, 114039. [CrossRef]
4. He, P.; Fang, Q.; Jin, H.; Ji, Y.; Gong, Z.; Dong, J. Coordinated design of PSS and STATCOM-POD based on the GA-PSO algorithm to improve the stability of wind-PV-thermal-bundled power system, *Int. J. Electr. Power Energy Syst.* **2022**, *141*, 108208. [CrossRef]
5. Kaliaperumal Rukmani, D.; Thangaraj, Y.; Subramaniam, U.; Ramachandran, S.; Madurai Elavarasan, R.; Das, N.; Baringo, L.; Imran Abdul Rasheed, M. A New Approach to Optimal Location and Sizing of DSTATCOM in Radial Distribution Networks Using Bio-Inspired Cuckoo Search Algorithm. *Energies* **2020**, *13*, 4615. [CrossRef]
6. Tariq, M.; Zaheer, H.; Mahmood, T. Modeling and Analysis of STATCOM for Renewable Energy Farm to Improve Power Quality and Reactive Power Compensation. *Eng. Proc.* **2021**, *12*, 44. [CrossRef]
7. Bharadwaj, A.; Maiti, S.; Dhal, N.; Chakraborty, S.; Pillai, S.K. Chapter 10—E-STATCOM (energy storage+STATCOM): A solution to integrate large-scale wind farms into the grid at medium and high power levels. In *Power Quality in Modern Power Systems*; Sanjeevikumar, P., Sharmeela, C., Holm-Nielsen, J.B., Sivaraman, P., Eds.; Academic Press: Cambridge, MA, USA, 2021; pp. 283–310, ISBN 9780128233467. [CrossRef]
8. Perera, S.; Elphick, S. Chapter 2—Steady-state voltage in low voltage networks. In *Applied Power Quality*; Perera, S., Elphick, S., Eds.; Elsevier: Amsterdam, The Netherlands, 2023; pp. 19–48. ISBN 9780323854672. [CrossRef]

9. Battistelli, C.; Monti, A. Chapter 5—Dynamics of modern power systems. In *Converter-Based Dynamics and Control of Modern Power Systems*; Monti, A., Milano, F., Bompard, E., Guillaud, X., Eds.; Academic Press: Cambridge, MA, USA, 2021; pp. 91–124. ISBN 9780128184912. [CrossRef]
10. He, L.; Lu, Z.; Geng, L.; Zhang, J.; Li, X.; Guo, X. Environmental economic dispatch of integrated regional energy system considering integrated demand response. *Int. J. Electr. Power Energy Syst.* **2020**, *116*, 105525. [CrossRef]
11. Ranamuka, D.; Muttaqi, K.M.; Sutanto, D. Flexible AC Power Flow Control in Distribution Systems by Coordinated Control of Distributed Solar-PV and Battery Energy Storage Units. *IEEE Trans. Sustain. Energy* **2020**, *11*, 2054–2062. [CrossRef]
12. Patnaik, B.; Swain, S.C.; Dash, R.K. An Experimental Analysis of Solar PV on Higher Concentration of Methane. In Proceedings of the 2022 IEEE India Council International Subsections Conference (INDISCON), Bhubaneswar, India, 15–17 July 2022; pp. 1–5. [CrossRef]
13. Sera, D.; Kerekes, T.; Teodorescu, R.; Blaabjerg, F. Improved MPPT algorithms for rapidly changing environmental conditions. In Proceedings of the 2006 12th International Power Electronics and Motion Control Conference, Portoroz, Slovenia, 30 August–1 September 2006; pp. 1614–1619.
14. Narsingoju, K.; Busa, V.; Kumar, G.V. Simulation analysis of maximum power control of photovoltaic power system. *Int. J. Adv. Electr. Electron. Eng.* **2012**, *1*, 9–14.
15. Patnaik, B.; Swain, S.C.; Dash, R. A Study on Effect of GHG on the Performance of Grid Connected Solar PV System. In Proceedings of the 2022 IEEE India Council International Subsections Conference (INDISCON), Bhubaneswar, India, 15–17 July 2022; pp. 1–4. [CrossRef]
16. Sakib, N.; Kabir, M.W.; Subbir, M.; Alam, S. A comparative study of flower pollination algorithm and bat algorithm on continuous optimization problems. *Int. J. Appl. Inf. Syst.* **2014**, *7*, 13–19. [CrossRef]
17. Yang, B.; Zhong, L.; Zhang, X.; Shu, H.; Yu, T.; Li, H.; Jiang, L.; Sun, L. Novel bio-inspired memetic salp swarm algorithm and application to MPPT for PV systems considering partial shading condition. *J. Clean. Prod.* **2019**, *215*, 1203–1222. [CrossRef]
18. Kumar, C.; Rao, R. A novel global MPP tracking of a photovoltaic system based on whale optimization algorithm. *Int. J. Renew. Energy Dev.* **2016**, *5*, 225–232. [CrossRef]
19. Mohanty, S.; Subudhi, B.; Ray, P.K. A new MPPT design using grey wolf optimization technique for photovoltaic system under partial shading conditions. *IEEE Trans. Sustain. Energy* **2016**, *7*, 181–188. [CrossRef]
20. Mansoor, M.; Feroz, Mirza, A.; Ling, Q. Harris hawk optimization-based MPPT control for PV systems under partial shading conditions. *J. Clean. Prod.* **2020**, *274*, 122857. [CrossRef]
21. El-Helw, H.M.; Magdy, A.; Marei, M.I. A hybrid maximum power point tracking technique for partially shaded photovoltaic arrays. *IEEE Access* **2017**, *5*, 11900–11908. [CrossRef]
22. Shen, H.; Xu, L.; Xu, Y.; Cao, J. A novel hybrid PSO-LSTM approach for improving MPPT performance of PV system under partially shaded conditions. *Sol. Energy* **2019**.
23. Kong, W.C.; Dong, Z.Y.; Jia, Y.W.; Hill, D.J.; Xu, Y.; Zhang, Y. Short-Term Residential Load Forecasting Based on LSTM Recurrent Neural Network. *IEEE Trans. Smart Grid* **2019**, *10*, 841–851. [CrossRef]
24. Ali, A.N.; Saied, M.H.; Mostafa, M.Z.; Abdel-Moneim, T.M. A survey of maximum PPT techniques of PV systems. In Proceedings of the 2012 IEEE Energytech, Cleveland, OH, USA, 29–31 May 2012; pp. 1–10.
25. Abd-Elazim, S.M.; Ali, E.S. Imperialist competitive algorithm for optimal STATCOM design in a multimachine power system. *Int. J. Electr. Power Energy Syst.* **2016**, *76*, 136–146. [CrossRef]
26. Ballaji, A.; Dash, R.; Subburaj, V.; Kalvakurthi, J.R.; Swain, D.; Swain, S.C. Design & Development of MPPT Using PSO with Predefined Search Space Based on Fuzzy Fokker Planck Solution. *IEEE Access* **2022**, *10*, 80764–80783. [CrossRef]
27. Ramadan, A.; Kamel, S.; Hassan, M.H.; V´eliz, T.M.; Eltamaly, A.M. Parameter Estimation of Static/Dynamic Photovoltaic Models Using a Developed Version of Eagle Strategy Gradient-Based Optimizer. *Sustainability* **2021**, *13*, 13053. [CrossRef]
28. Rivera, D.; Guillen, D.; Mayo-Maldonado, J.C.; Valdez-Resendiz, J.E.; Escobar, G. Power grid dynamic performance enhancement via STATCOM data-driven control. *Mathematics* **2021**, *9*, 2361. [CrossRef]